BRAKE VALVE TIMING AND FUEL INJECTION: A UNIFIED ENGINE TORQUE ACTUATOR FOR HEAVY-DUTY VEHICLES

L.Moklegaard, M. Druzhinina [1] and A. G. Stefanopoulou
University of California, Santa Barbara

Abstract

A unified engine torque actuator for heavy-duty vehicles is developed in this paper. Based on averaging and identification of the instantaneous torque response for changes in brake valve timing and fuel flow, we derive a nonlinear, control oriented engine model of a six cylinder, 350 Hp turbocharged diesel engine, equipped with a compression brake. This work bridges the gap between the detailed crank angle based models developed in the engine design community, and the first order lag representation of diesel engine torque response used in the vehicle dynamics community. Moreover, we integrate the compression brake actuator with the service brakes and design a PI-controller that emulates the driver's actions to avoid "runaways" during descends on grades. The controller simply uses the engine speed measurement to activate the service brakes only when needed.

1 Introduction

Heavy duty vehicles ($HDVs$) are an essential part of our nation's economy. In 1996, the intercity trucking industry accounted for $176.8 billion in revenues and over 2.9 million jobs [8]. The past few years there has been an increased activity in truck safety related issues. A critical safety issue for HDVs is the vehicle retarding capability. The need for higher brake power is addressed by truck manufacturers and fleet managers by the development of various retarding mechanisms. The compression brake is an engine retarding mechanism, in which the internal combustion engine dissipates the vehicle kinetic energy by compressing the cylinder air charge. This is achieved by a secondary opening of the exhaust valve approximately at the end of the compression stroke to permit the compressed air charge to escape to the exhaust manifold [2]. We call the secondary opening of the exhaust valve v_{cb}, and define it as crank angle degree from TDC_1, as seen in Figure 1. The concept of compression braking was introduced by Cummins in 1966, and typically, depends on an add-on device that opens the exhaust

valve at fixed degrees with respect to the piston motion. Considerable effort is dedicated in optimizing the fixed valve timing to achieve maximum retarding power for all engine speed, load and environmental conditions. The fixed brake valve timing mechanism is an
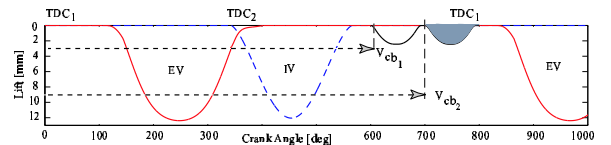

Figure 1: Valve timing shown in crank angle domain. The secondary opening of the exhaust valve associated with the minimum and maximum brake valve timings is also shown.

on-off device and produces a fixed brake torque for a given engine speed. However, for applications in Intelligent Transportation Systems (ITS) full control over the brake valve timing is desirable. A continuously varying brake valve timing allows smooth changes in the compression brake torque response while maintaining constant engine speed. This variability can be used in various HDV applications such as speed regulation, brake-by-wire systems, cruise control, and finally, vehicle-following maneuvers. Moreover, full integration of the compression brake with the service brakes (drum or disc brakes on the vehicle wheel rim) can be achieved. Due to the potential benefits, many engine manufacturers are striving for variable compression braking effort. Work is summarized by Jacobs variable brake valve timing [6], Cummins' discrete cylinder brake valve actuator [12], and Volvo's variable compression braking with exhaust throttle actuator [1].

Identifying the mean-value engine torque responses to changes in brake valve timing and fuel level, for different engine and drivetrain operating conditions, is the focus this paper. A low order input-output engine model is developed with an input signal from -100 to 100 that corresponds to a scaled fuel command if it has positive values, or a scaled brake valve timing if it has negative values. This work bridges the gap between the detailed crank angle based model developed in the engine design community, and the first order lag repre-

sentation of diesel engine torque response used in the vehicle dynamics community.

The low order, mean-value engine model is derived by applying input-output identification techniques on an event-based averaged signal of the instantaneous torque response developed in ([10]). The inputs to the mean-value model are fuel flow, brake valve timing and engine speed, while shaft torque is the output. It is worth mentioning here that most vehicle control problems use a simplified longitudinal model to develop the throttle (fuel) and braking control algorithms by considering only the dominant dynamics of the process [7, 9]. This was largely achieved due to the clear separation between (i) the fast dynamics of the angular wheel velocity and the fueling system, (ii) the moderate dynamics ($\tau \approx 0.2$ sec) of the intake manifold, engine speed, and turbocharger rotor, and finally, (iii) the slow dynamics of the vehicle velocity. In this paper we investigate if the engine torque response to variable compression braking can be approximated and if similar simplifications are acceptable from a control design perspective.

To this end, we use the identified mean-value model to design a low order controller for vehicle speed regulation. Conventional compression brakes are used to stabilize or to reduce vehicle speed on a long decline after a series of complicated actions performed by the vehicle driver. In this paper, we integrate the compression brake actuator with the service brakes and design a PI-controller that emulates the driver's actions to avoid "runaways" during descends on grades. The controller simply uses the engine speed measurement to activate the service brakes only when needed.

The paper is organized as follows. The crank angle based engine model developed in [10] is the basis for the low order identification, hence we review it in Section 2. In Section 3, we discuss the averaging and system identification techniques we use to derive the reduced engine model in Section 4. In Section 5, we combine the unified engine torque actuator with the HDV longitudinal dynamics. In the same section, we analyze the stability of the equilibrium descending speed. Furthermore, we compare qualitatively the possible equilibria for the experimental brake and the 1966 engine brake reported in [2]. The controller design and simulation results are shown in Section 6, while a sensitivity analysis is presented in Section 7.

2 Crank Angle Based Model

The turbocharged, compression ignition internal combustion (diesel) engines is the preferred powerplant for HDVs. Unlike gasoline engines, diesel engines operate unthrottled, hence, the pistons do not have to work against intake manifold vacuum during the in-

take stroke. This, combined with very lean mixtures of fuel and air, contributes to the increased fuel economy and to the decreased natural retarding power. To augment to the retarding capabilities of diesel engines, a compression braking mechanism is added.

A diesel engine equipped with a compression braking mechanism operates in either combustion, or in braking mode. The difference between the two modes is illustrated in Figure 2, through a plot of cylinder pressure versus cylinder volume (PV-diagram). The work generated or absorbed by the pistons is given by the integral $\oint p_{cyl} dV_{cyl}$. In the combustion mode (dashed line), fuel is injected into the cylinder (start-of-injection, SOI) close to top-dead-center (TDC) in the compression stroke. The fuel ignites due to the high cylinder pressure and generates positive work due to the clock-wise direction of the PV-trace in Figure 2. In the braking mode (solid line), on the other hand, fuel injection is inhibited, and the compressed air is released into the exhaust manifold through a secondary opening of the exhaust valve (brake-valve-opening, BVO) close to TDC. The kinetic energy absorbed by the pistons during the compression stroke is dissipated as heat in the exhaust manifold. The total work during the engine cycle is here negative, evident from the counter-clockwise direction of the PV-trace in Figure 2 (solid line).
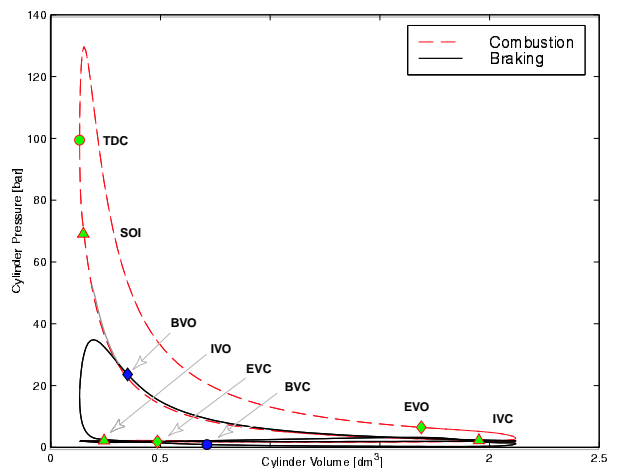

Figure 2: **PV**-diagram for unified engine torque actuator (adapted from [10]).

To analyze and to quantify the effects of the brake valve opening v_{cb}, a novel nonlinear, crank angle based simulation model for a six cylinder, 350 Hp diesel engine is developed in [10]. The model is based on physical equations and static engine maps provided by manufacturers. The model is capable of describing the intrinsic interactions between individual cylinder in-

take and exhaust processes, and turbocharger dynamics during combustion and braking modes and the transition between those modes.

In particular, the intake and exhaust manifolds, and the cylinders are modeled as plenums with spatially homogeneous pressure and temperature distributions. The plenum model is based on the conservation of mass and energy principles, and the assumption of the ideal gas law. The mass gas flow through all the plenums and valves are based on a quasi-steady model of an one-dimensional, steady, compressible flow of an ideal gas through an orifice [5]. The turbocharger speed is based on the conservation of energy on the turbocharger shaft, while the turbine and compressor mass air flow and efficiency are based on static maps provided by the manufacturer. Furthermore, the apparent burn fuel rate is identified based on crank angle resolved cylinder pressure at different operating conditions for speed and load. The individual instantaneous cylinder torque is based on cylinder pressure and piston motion using an idealized slider-crank mechanism. The total instantaneous shaft torque is based on the summation of individual instantaneous cylinder torques.

3 Averaging and Identification of Torque

Simulation results in [10] demonstrate that the dominant torque dynamics are in the order of engine cycles (1 second) and not in the order of crank angles (10^{-4} seconds). Moreover, the complexity of the 23 states in the crank angle based model precludes the development of control algorithms for in-vehicle applications. To manage this complexity and to extract the dominant cycle-to-cycle dynamical behavior, we average the crank angle based instantaneous torque response. The instantaneous torque response is sampled every 2 crank angle degrees and then averaged over a fundamental cylinder event (120 crank angle degrees for the six cylinder experimental engine).

Using the event-based averaged torque signal, we apply system identification techniques to a series of output perturbations due to small input step changes around various equilibrium points. Note here that the "first" data point in the averaged torque signal is sensitive to the choice of the window of the crank angle resolved data. The "first" data point refers to the averaged torque data point after the input step change. All the other averaged torque data points are robust with respect to the data window.

Our goal is to approximate the nonlinear averaged torque using a set of linear time invariant (LTI) systems in the neighborhood of selected operating points that span the input excitation domain. Specifically, we generate LTI systems that represent both combus-

tion and braking modes by a series of averaged torque simulations in response to fuel flow, brake valve timing and engine speed steps. These series of simulation serve as input-output identification experiments. The output-error model in the System Identification Toolbox in Matlab is used to extract the parameters of the LTI systems that capture the input-output behavior of each identification experiment.

To facilitate the development of a nonlinear controller, we develop a reduced engine model by interpolating the parameters of the series of LTI systems with polynomials of engine speed and the unified engine signal (scaled fuel flow and scaled brake valve timing). Developing the polynomial regression of the LTI system parameters requires constant model order for all the LTI system approximations. A first order dynamical system is used as the target LTI approximation for all identification experiments. This is a challenging task because each engine mode is governed by different dynamics. In particular, the step responses to changes in engine speed while in braking mode, are more accurately approximated with second order systems than with first order ones. Furthermore, efficient system identification methodologies for a fixed structure (order) are not readily available. We, thus obtain some approximations by applying the classical identification rule of the rise time of a first order lag.

A few examples of the averaging and system identification we performed for braking, and combustion modes are shown in Figure 3 and 4, respectively. For braking mode, we show in Figure 3, the torque responses to: (i) a step change in brake valve timing v_{cb}, from 685 to 678 degrees, for a constant engine speed $\omega = 157$ rad/sec, and (ii) a step change in ω, from 157 to 165 rad/sec, for a constant $v_{cb} = 685$ degrees.
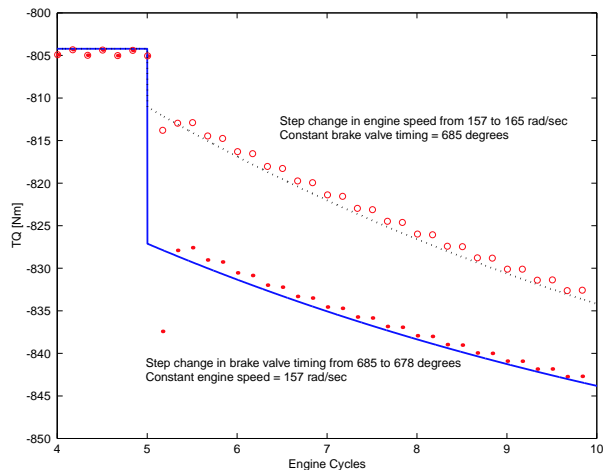

Figure 3: Averaged (dots) and identified torque response to: step in brake valve timing (solid line), and engine speed (dotted line).

In Figure 4, on the other hand, we show two examples for the combustion mode. Specifically, we show the torque responses to: (i) a step change in fuel flow v_f, from 10 to 11 g/sec, for a constant engine speed $\omega = 157$ rad/sec, and (ii) a step change in ω, from 157 to 165 rad/sec, for a constant $v_f = 10$ g/sec.
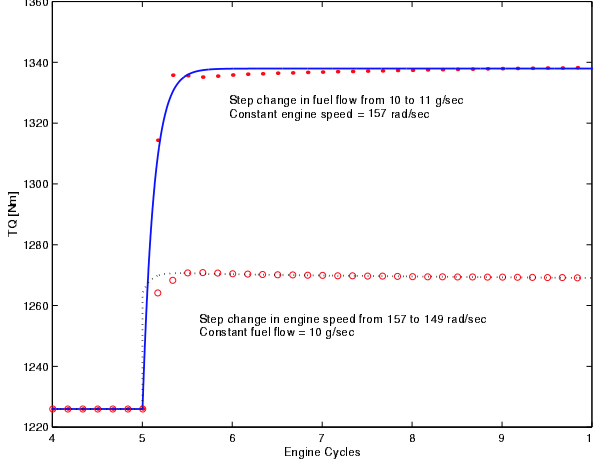

Figure 4: Averaged (dots) and identified torque response to step in: fuel flow (solid line) and engine speed (dotted line).

4 Reduced Engine Model

Based on the extracted family of first-order, local linear time invariant models, we develop a reduced order, nonlinear dynamic model of the engine as a unified torque actuator. In accordance with engine torque identification process described in Section 3, the dynamics describing the combustion mode mirror the dynamics describing the braking mode. Using standard regression techniques, we employ the following polynomial parametrization for the unified torque $TQ(t)$:

$$TQ(t) = \mathcal{P}_{TQ}(\tilde{\omega}(t), W(t)). \qquad (1)$$

Here, $\tilde{\omega}(t)$ is characterized by the following dynamics:

$$
\begin{aligned}
\tilde{\omega}(t) &= \Delta\tilde{\omega}(t) + \omega_{nom} \\
\tau_\omega \frac{d}{dt}(\Delta\tilde{\omega}(t)) &= -\Delta\tilde{\omega}(t) + \Delta\omega(t) + c_\omega \frac{d}{dt}(\Delta\omega(t)), \quad (2)
\end{aligned}
$$

where ω_{nom} is the nominal engine speed, and $\Delta\omega$ is the deviation of the engine speed ω, from nominal engine speed; i.e. $\Delta\omega(t) = \omega(t) - \omega_{nom}$. $W(t)$ is the unified signal in the range between -100 and 100 percent, which takes the value $W^F(t)$ when the engine is in combustion mode, and $W^B(t)$ when the engine is in braking mode.

The dynamics of $W(t)$ is described by the following equations:

$$
\begin{aligned}
W(t) &= \Delta W(t) + W_{nom}, \\
\tau \frac{d}{dt}(\Delta W(t)) &= -\Delta W(t) + \Delta v(t) + c\frac{d}{dt}(\Delta v(t)) \quad (3)
\end{aligned}
$$

where W_{nom} refers to a nominal operating condition for the engine; i.e. W_{nom}^F corresponds to a nominal fuel flow, while W_{nom}^B corresponds to a nominal brake valve timing.

The input Δv, in (3), denotes fuel flow from the fuel pump actuator when the engine is in combustion mode, and brake valve timing when the engine is in braking mode. The equation that describes the dynamics of Δv, is given by:

$$\tau_a \frac{d}{dt}(\Delta v(t)) = -\Delta v(t) + \Delta u(t), \qquad (4)$$

where $\Delta u(t)$ is the deviation of the output of the in-vehicle controller u(t) from the nominal signal W_{nom}; i.e. $\Delta u(t) = sat(u(t)) - W_{nom}$. (A PI-controller for braking only is described in details in Section 6). Note that the combustion operating mode is activated when $u(t)$ is positive; i.e. $u \geq 0$, and the braking mode is activated when $u(t)$ is negative, i.e. $u < 0$. The minimum and maximum values of u that define $sat(u(t))$ are -100, and 100, respectively.

The time constants τ, τ_ω, and τ_a, for the systems in (3), (2), and (4), respectively, and the zeros c and c_ω of the systems in (3) and (2), respectively, are obtained for different operating modes by the following set of polynomials of nominal engine speed ω_{nom}, and nominal signal W_{nom}:

$$
\tau = \begin{cases} \mathcal{P}_{F1}(\omega_{nom}, W_{nom}^F), & \text{for combustion mode} \\ \mathcal{P}_{B1}(\omega_{nom}, W_{nom}^B), & \text{for braking mode} \end{cases}
$$

$$
c = \begin{cases} \mathcal{P}_{F2}(\omega_{nom}, W_{nom}^F), & \text{for combustion mode} \\ \mathcal{P}_{B2}(\omega_{nom}, W_{nom}^B), & \text{for braking mode} \end{cases}
$$

$$
\tau_\omega = \begin{cases} \mathcal{P}_{F3}(\omega_{nom}, W_{nom}^F), & \text{for combustion mode} \\ \mathcal{P}_{B3}(\omega_{nom}, W_{nom}^B), & \text{for braking mode} \end{cases}
$$

$$
c_\omega = \begin{cases} \mathcal{P}_{F4}(\omega_{nom}, W_{nom}^F), & \text{for combustion mode} \\ \mathcal{P}_{B4}(\omega_{nom}, W_{nom}^B), & \text{for braking mode} \end{cases}
$$

$$
\tau_a = \begin{cases} \mathcal{P}_{F5}(\omega_{nom}, W_{nom}^F), & \text{for combustion mode} \\ \mathcal{P}_{B5}(\omega_{nom}, W_{nom}^B), & \text{for braking mode} \end{cases}
$$

The unified engine torque given in (1) is shown Figure 5. Positive values on the x-axis indicates fuel flow, and negative values indicates brake valve timing. An interesting observation is that the rate of change for the brake torque changes sign for high valve timings in the reduced order model. However, the torque sign reversal is eliminated by imposing a hardware constrain on the maximum value of W^B.

Typical step responses for the dynamics given by (2) and (3) are shown in Figure 6 for a set of nominal
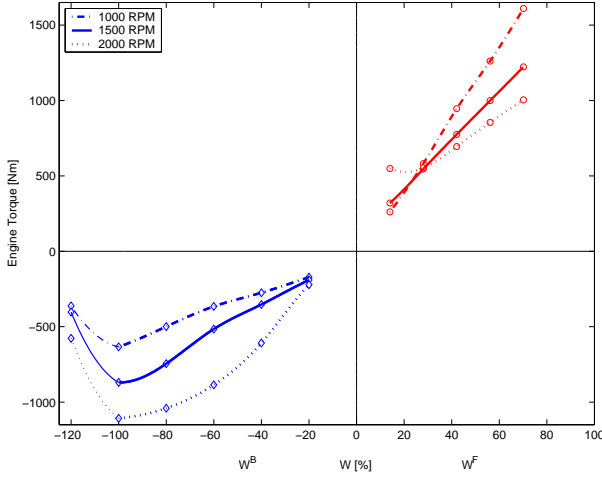
Figure 5: By combining fuel flow, and brake valve timing into one, we generate a map for the unified steady-state engine torque.

operating points. The normalization of the time scale is: $t_{norm} = \alpha t$, where $\alpha = 700$ for combustion, and $\alpha = 0.5$ for braking.
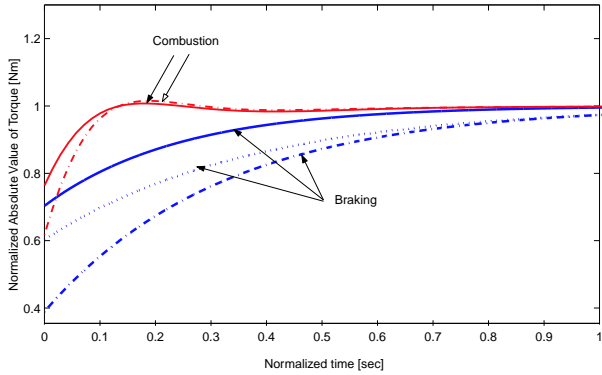

Figure 6: Step responses to a family of nominal operating conditions for braking and combustion modes.

5 Vehicle Dynamics and Equilibrium Analysis

A lumped parameter approximation of the vehicle, engine, and transmission is used in Newton's law. Specifically, the rate of change of engine speed ω, depends on the power that is generated and absorbed in the crank shaft:

$$J_T \omega \frac{d\omega}{dt} = P_e - P_{sb} + P_\beta - P_a - P_r, \qquad (5)$$

where J_T is the total vehicle inertia reflected to the engine shaft. $P_e = TQ\omega$ is the engine power generated or absorbed based on TQ calculated in (1). $P_{sb} = F_{sb}v$ is the retarding power due to the friction brake force

of F_{sb} applied on the wheel rim that travels with linear velocity v. The wheel rim linear velocity is equal to the vehicle speed $v = r_g\omega$, where the total gear ratio $r_g = \frac{r_w}{g_t g_{fd}}$ depends on the transmission gear ratio, g_t, the final drive gear ratio g_{fd}, and the wheel radius r_w. The power P_β, due to gravity for a vehicle of mass M, descending on a grade β; i.e. $\beta < 0$, with a speed v, is given by $P_\beta = -Mg\sin(\beta)v$. The vehicle natural retarding power depends on the aerodynamic drag, $P_a = C_a v^3$, and the rolling resistance, $P_r = \mu Mg\cos(\beta)v$, where the constants C_a and μ are associated with the aerodynamic and the rolling resistance coefficients, respectively.

Figure 7 shows a diagram of power versus engine speed that is used extensively in the trucking industry to find equilibrium descending engine speed ω^*, given a descending grade and the engine compression braking power. The equilibrium descending engine speed ω^*, is defined at the intersection of the retarding vehicle power $P_e - P_a - P_r$, with the power due to gravity P_β. This figure is informative because it depicts the allowable range of engine speed; it can be used for sizing the engine brake actuator based on a range of expected grades and vehicle loading conditions.
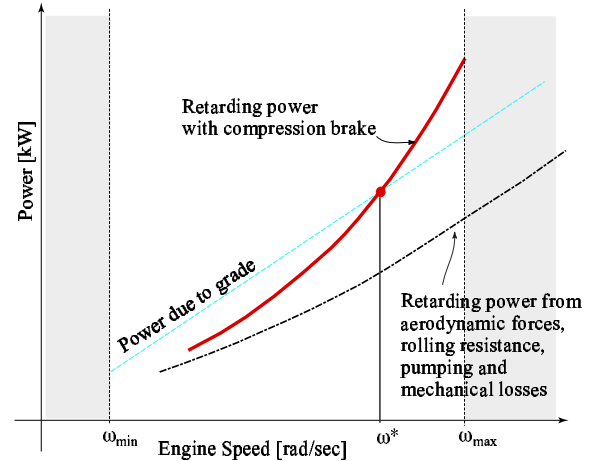

Figure 7: Vehicle braking power versus speed during a descent (adapted from [10]).

It is of interest to see how the compression brake technology has evolved since 1966, when it first was introduced to the transportation industry by Cummins [2]. Figure 8 shows how the equilibrium points ω_{66}, and ω_{99}, that define the engine descending speed, have changed from 1966 to 1999. The data for the curve denoted "Engine Brake, 1966," is adapted from [2], while the data for the curve denoted "Engine Brake, 1999," is based on the experimental Mack engine retarding power calculated from (1). First of all, the current descending engine speed is higher than the one attained in 1966; i.e. $\omega_{99} > \omega_{66}$. It is important to
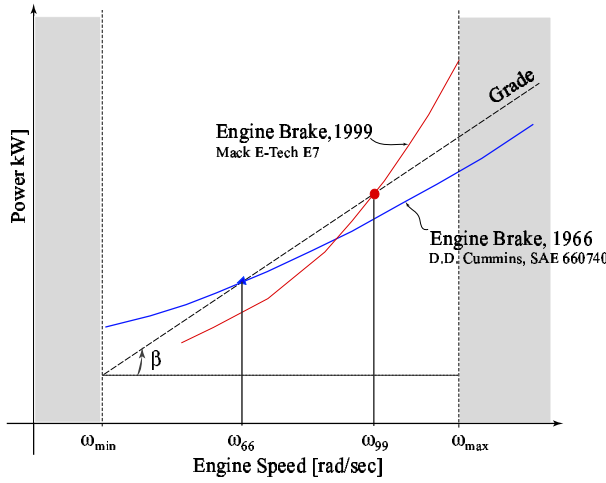
Figure 8: Figure show how a typical equilibrium point for vehicle speed has changed from ω_{66} in 1966, to ω_{99} in 1999 (adapted from [10]).

note that ω_{99} is a *stable* equilibrium point, while ω_{66} is *unstable*. The reason for this change in equilibrium stability is two fold. For low speed, the current braking system shows lower retarding power than the one from 1966. This is due to the reduced natural vehicle retarding power associated with reduction in mechanical losses, such as friction, pumping and aerodynamic drag. For high speed, on the other hand, the increase in braking power is most likely due to improvements in the actuator mechanism of the brake valve opening; i.e. the high pressure hydraulic mechanism that activates the secondary exhaust valve opening. The old technology could not support a consistent fast valve opening and closing for high engine speed. The combination of actuator and engine hardware improvements result in a higher, and stable equilibrium ω_{99}. Note here that safe operation at higher equilibrium descending speed is preferred due to a potential increase of average vehicle speed and, consequently, a decrease in HDV trip duration.

6 Controller Design and Simulations

In this section, we employ a classical PI-controller design to regulate the vehicle speed $v(t)$ to the desired constant vehicle speed v_d, during a long descent down a grade. Since the engine rotational speed ω, is related to the vehicle speed by $v = \omega r_g$, this ensures that $\omega \to \omega_d(t)$ as long as the gear is constant. Additionally, we assume that the braking with compression brakes is preferable, because we want to minimize the use of service brakes to potentially reduce the wear of

the friction pads in the brakes.

The PI-controller for *braking* only is given by:

$$u(t) = k_b \left((\omega_d - \omega(t)) + \frac{1}{\tau_b} \int_0^t (\omega_d - \omega(\tau))d\tau \right) + W_{nom}^B \quad (6)$$

The gains of the controller are tuned using Ziegler and Nichols' classical approach [11]. Recall that the output of (6), $u(t)$, is the input to the dynamics in (4), (see Section 2 for details).

Coordination of the compression brake with the friction brakes is achieved using the following P-controller:

$$u_{sb}(t) = -k_{s1}(u - sat_{min}(u)) + k_{s2}(\omega - sat_{max}(\omega)), \quad (7)$$

where u_{sb}, is the input to the service brake actuator. Based on (7), the service brakes are activated when the control signal for compression brake (6) reaches its minimum value $sat_{min}(u) = -100$, or when the engine speed exceeds a safe operating level, $sat_{max}(\omega) = 250$ rad/sec. The control strategy based on (6)-(7) assigns high priority to the compression brake and uses the service brakes only when absolutely necessary. This reduces the use of conventional service brakes, thus potentially reduce maintenance costs.

In Figures 9 and 10, we demonstrate the closed-loop system performance for two critical driving scenarios. To assess the improvements we achieve using the coordinated braking controller scheme (CBC) based on (6)- (7), we simulate the same driving scenarios with the compression brake disabled, i.e., using PI-control on the service brakes only (SBO):

$$u_{sbo}(t) = k_{s1} \left((\omega_d - \omega(t)) + \frac{1}{\tau_s} \int_0^t (\omega_d - \omega(\tau))d\tau \right), \quad (8)$$

where u_{sbo}, is the input to the service brake actuator.

To quantify the improvements we achieve using the CBC scheme, we define the following performance index:

$$I = \int_0^{t_s} u_{sb}(\tau)^2 d\tau, \quad (9)$$

where the settling time t_s, is defined as the time required for the service brake actuator signal u_{sb}, to reach and remain inside a band whose width is equal to $\pm 5\%$ of the new steady state value [11]. The performance index, I is a measure of how much the service brakes are used and we use it together with the settling time t_s to refine the PI-controller parameters we obtained using the Ziegler and Nichols' method. The set of gain's we finally choose achieves a reasonable vehicle response for wide range of operations.

The first driving scenario shown in Figure 9, illustrates a HDV in braking mode, descending on a constant grade, $\beta = 3$ degrees (dash-dotted line in the upper plot). The total gear ratio r_g (here, corresponding

to the fifth gear), is kept constant throughout the simulations. After two seconds, we command a step change in desired engine speed from 157 to 149 rad/sec (lower plot). After an initial overshoot of approximately seven percent, the engine speed is regulated to its new desired level after six seconds. In the CBC scheme, the service
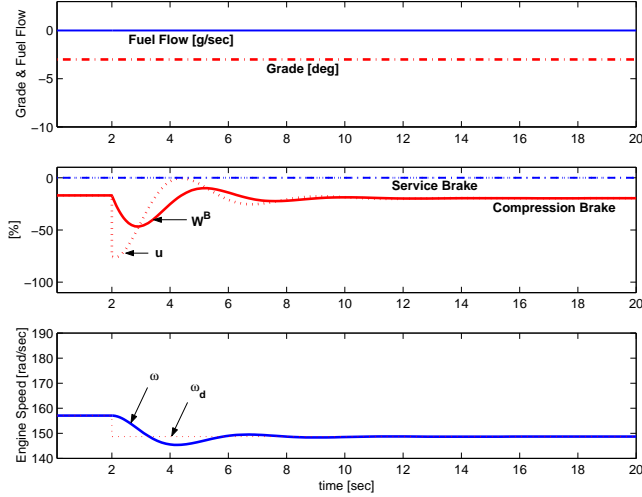

Figure 9: Step change in desired engine speed from 157 to 149 rad/sec when operating in braking mode.

brakes are not used at all, as we see in the middle plot. Consequently, both the settling time and the performance index are zero. The same driving scenario using the SBO scheme results in a settling time $t_s = 6.5$ seconds, while the performance index I, in (9) is 49.3.

The other critical driving scenario, shown in Figure 10, illustrates the HDV during a transition from combustion to braking mode, with a constant engine speed $\omega = 157$ rad/sec. The vehicle is initially cruising on a flat terrain with a fuel flow $v_f = 1.9$ g/sec (solid line in the upper plot). After two seconds, the vehicle encounters a grade change from $\beta = 0$ to -9 degrees (dash-dotted line in upper plot). As seen in the middle plot, both the compression brake and the service brakes are employed to maintain the engine speed. After an initial overshoot of approximately 16 percent, the engine speed is regulated to desired level after 12 seconds. In this driving scenario, the performance index I, in (9) is 17 times higher for the SBO scheme than for the CBC scheme. In addition, the settling time t_s, is reduced by more than 40 percent, from 7.3 to 5.2 seconds, using the coordination of service brakes and compression brake. These substantial reductions of the index I, and the settling time t_s, can potentially result in reduction of wear and tear of the friction pads in the service brakes.

In Figure 11 we show the corresponding phase plots for driving scenarios one and two. The figure demonstrate the importance of taking the dynamics into ac-
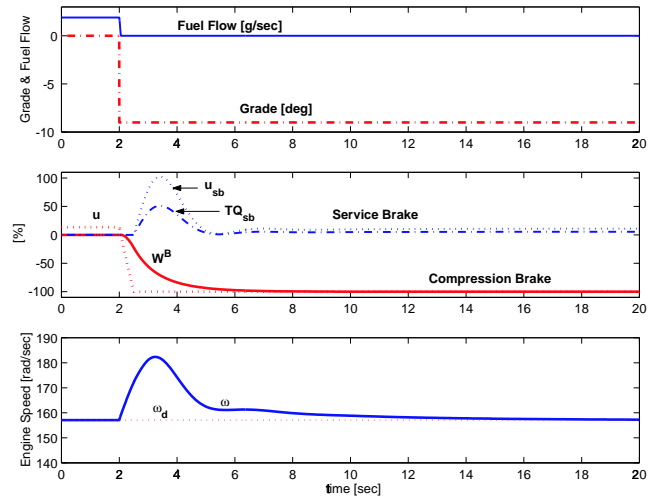

Figure 10: Switching from combustion to braking mode.
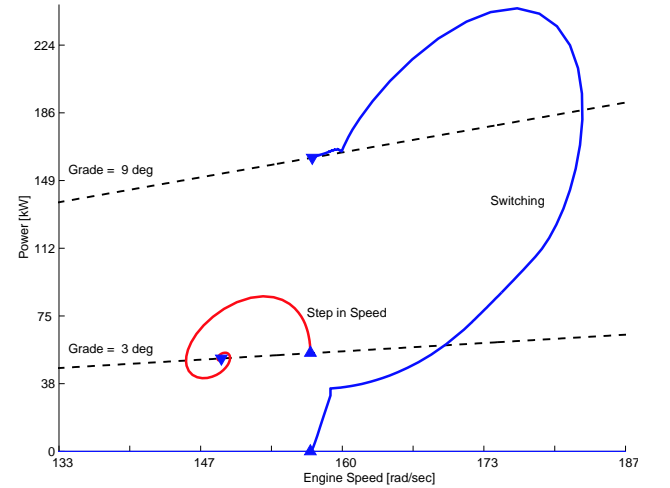
count when we perform engine speed equilibrium analysis.

Figure 11: Phase plot for driving scenario one and two.

7 Sensitivity Analysis

In Figure 12, we show the engine speed time responses for three different vehicle masses and gear ratios, due to a unit step change in u, for a $u < 0$. There is a significant sensitivity to changes in gear ratios as seen in the upper plot in Figure 12. In fact, the time constant for the system varies from 22 seconds when using the first gear, to about 140 seconds when using the tenth gear.

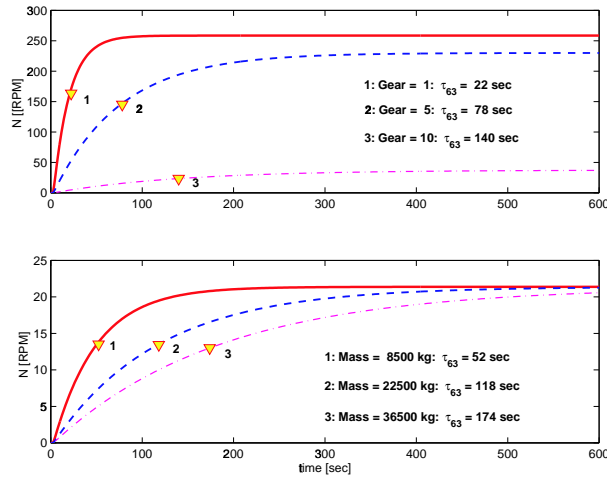Variations in the vehicle mass also greatly influence the vehicle dynamics. The mass for the system can

Figure 12: Engine speed time response to step change in brake valve timing.

vary as much as 400 percent from being tractor only, to being a system of tractor and trailer(s) with maximum allowable load. The lower plot in Figure 12, shows that the time constant τ_{63}, increases from 52 seconds for tractor alone to approximately 174 seconds for the combination of a tractor and fully loaded trailer(s).

It is also of interest to investigate how much a unit step change in grade affects the engine speed time response for the same three vehicle masses and gear ratios. This is shown in Figure 13. In the upper plot
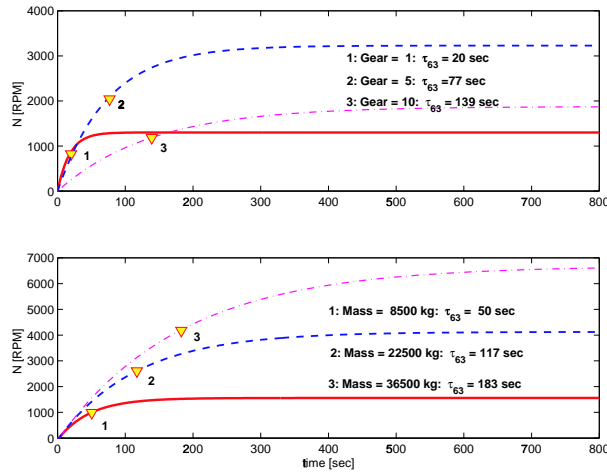

Figure 13: Engine speed response to step change in grade.

of this figure, we observe a non-monotonic behavior in the steady-state engine speed. The reason for this is that the aerodynamic drag force has a quadratic dependency on vehicle speed, $F_a = Cv^2$. The time constants, on the other, do show a monotonic behavior in accordance with the other time constants in Figure 12

and 13. Here, τ_{63}, varies from approximately 20 to 139 seconds for gear one and ten, respectively.

For variations in mass, as shown in the lower plot in Figure 13, the time constant varies from 50 seconds when the system consists of trailer alone, to approximately 183 seconds for a system of tractor and fully loaded trailer(s).

Our sensitivity analysis indicates the need for non-linear control design, and this is pursued [3] and in [4]. Specifically, the authors are using the model reference adaptive control (MRAC) approach in [3], and the speed gradient method in [4] to address the HDV speed regulating and tracking problems during large parameter deviations and unknown road conditions.

References

[1] P. Carlstrom. "Volvo High Power Engine Brake". Retrieved on: http:/www.truck.volvo.se, May 1999.

[2] D. D. Cummins. "The Jacobs Engine Brake Application and Performance". *SAE*, (660740), 1966.

[3] M. Druzhinina, L. Moklegaard, and A. G. Stefanopoulou. "Compression Braking Control for Heavy-Duty Commercial Vehicles". *Submitted to ACC*, 2000.

[4] M. Druzhinina, L. Moklegaard, and A. G. Stefanopoulou. "Speed Gradient Approach for Longitudinal Control of Heavy Duty Vehicles equipped with Compression Brake ". *Submitted to AVEC*, 2000.

[5] J. B. Heywood. *Internal Combustion Engine Fundamentals*. McGraw-Hill, 1988.

[6] H. Hu, J. Vorih, and M. Israel. "Lost-Motion VVT Diesel Engine Retarder". *Automotive Engineering International*, Jan, 1998.

[7] P. Ioannou and Z. Xu. "Throttle and Brake Control Systems for Automatic Vehicle Following. Technical Report UCB-ITS_PRR-94-10, PATH Research Report, 1994.

[8] John Deere. "Sharing the Road Media Group". Retrieved on: http://www.deere.com/truckerimage/.

[9] D. H. McMahon, J. K. Hedrick, and S. E. Shladover. "Vehicle Modelling and Control for Automated Highway Systems", 1990.

[10] L. Moklegaard, J. Schmidt, and A. G. Stefanopoulou. "Transition from Combustion to Variable Compression Braking". *Proceedings for the 2000 SAE World Congress"*, 2000.

[11] D. E. Seborg, T. F. Edgar, and D. A. Mellichamp. *Process Dynamics and Control*. John Wiley & Sons, Inc., 1989.

[12] Jacobs Vehicle System. "Intebrake Engine Braking Systme for Signature 600". Retrieved on: http:/www.jakebrake.com/products/engine, March 1999.